DOI: 10.1534/genetics.105.040634

Dissection of Arp2/3 Complex Actin Nucleation Mechanism and Distinct Roles for Its Nucleation-Promoting Factors in *Saccharomyces cerevisiae*

Jessica L. D'Agostino and Bruce L. Goode[1]

Department of Biology and Rosenstiel Basic Medical Science Research Center, Brandeis University, Waltham, Massachusetts 02454

Manuscript received January 8, 2005
Accepted for publication May 31, 2005

ABSTRACT

Actin nucleation by the Arp2/3 complex is under tight control, remaining inactive until stimulation by nucleation-promoting factors (NPFs). Although multiple NPFs are expressed in most cell types, little is known about how they are coordinated and whether they perform similar or distinct functions. We examined genetic relationships among the four *S. cerevisiae* NPFs. Combining *las17*Δ with *pan1-101* or *myo3*Δ*myo5*Δ was lethal at all temperatures, whereas combining *pan1-101* with *myo3*Δ*myo5*Δ showed no genetic interaction and *abp1*Δ partially suppressed *las17*Δ. These data suggest that NPFs have distinct and overlapping functions *in vivo*. We also tested genetic interactions between each NPF mutant and seven different temperature-sensitive *arp2* alleles and purified mutant Arp2/3 complexes to compare their activities. Two *arp2* alleles with mutations at the barbed end were severely impaired in nucleation, providing the first experimental evidence that Arp2 nucleates actin at its barbed end *in vitro* and *in vivo*. Another *arp2* allele caused partially unregulated ("leaky") nucleation in the absence of NPFs. Combining this mutant with a partially unregulated allele in a different subunit of Arp2/3 complex was lethal, suggesting that cells cannot tolerate high levels of unregulated activity. Genetic interactions between *arp2* alleles and NPF mutants point to Abp1 having an antagonistic role with respect to other NPFs, possibly serving to attenuate their stronger activities. In support of this model, Abp1 binds strongly to Arp2/3 complex, yet has notably weak nucleation-promoting activity and inhibits Las17 activity on Arp2/3 complex in a dose-responsive manner.

NUCLEATION of actin filament assembly is a key control point in the regulation of actin network formation. The Arp2/3 complex is one of two cellular factors (the other being formins) that recently have emerged as conserved actin nucleators in virtually all eukaryotes (Welch and Mullins 2002; Wallar and Alberts 2003). Actin nucleation by the Arp2/3 complex is critical for many cellular processes, including endocytosis, intracellular transport, and leading edge advancement during cell migration. The Arp2/3 complex is composed of seven subunits: Arp3, Arp2, p40/ARPC1, p35/ARPC2, p21/ARPC3, p19/ARPC4, and p15/ARPC5 (Machesky *et al.* 1994). Arp2 and Arp3 are ~46 and 39% identical to actin, respectively (Lees-Miller *et al.* 1992; Schwob and Martin 1992; Huang *et al.* 1996), and are predicted to directly nucleate actin polymerization. This is predicted on the basis of high degree of sequence and structural homology among Arp2, Arp3, and conventional actin, particularly at the barbed end of these proteins, *i.e.*, subdomains I and III (Kelleher *et al.* 1995; Robinson *et al.* 2001). However, this has not yet been demonstrated experimentally.

[1]*Corresponding author:* Rosenstiel Center, Department of Biology, Brandeis University, 415 South St., Waltham, MA 02454.
E-mail: goode@brandeis.edu

Purified Arp2/3 complex alone poorly nucleates actin assembly and requires the addition of a nucleation-promoting factor (NPF) for efficient nucleation. NPFs include members of the Wiskott-Aldrich syndrome protein (WASp)/SCAR/WAVE family, cortactin, Abp1, Pan1, and fungal type I myosins (Goode and Rodal 2001; Welch and Mullins 2002). In the crystal structure of bovine Arp2/3 complex, Arp2 and Arp3 are well separated, suggesting that it is an inactive conformation (Robinson *et al.* 2001). Addition of WASp to Arp2/3 complex induces major structural rearrangements that drive Arp2 and Arp3 closer together, presumably to form a pseudoactin dimer that provides a template for actin nucleation (Goley *et al.* 2004; Rodal *et al.* 2005a). In addition to stabilizing this closed Arp2/3 conformation, WASp must present an actin monomer to the barbed ends of Arp2 and/or Arp3 (Welch and Mullins 2002).

One question that has arisen from the identification of multiple NPFs is whether they have similar or distinct cellular functions and mechanisms of activating the Arp2/3 complex. Further, it is unclear how their activities are coordinated *in vivo*. Even in a relatively simple eukaryote like *Saccharomyces cerevisiae*, five different NPFs are expressed: Las17/Bee1, the homolog of WASp; Abp1; Pan1, the homolog of Eps15; and Myo3

and Myo5, two type 1 myosins (Li 1997; Evangelista *et al.* 2000; Lechler *et al.* 2000; Duncan *et al.* 2001; Goode *et al.* 2001). All of these NPFs localize to and function at cortical actin patches, which are dynamic sites of actin assembly and endocytosis, but their individual roles have remained elusive. Some NPFs, including cortactin and Abp1, are known to bind to actin filaments and lack any detectable actin monomer-binding affinity (Goode *et al.* 2001; Uruno *et al.* 2001; Weaver *et al.* 2001). These specialized properties have raised the possibility that Abp1 and cortactin may perform NPF functions distinct from members of the WASp/SCAR/WAVE family. Indeed, one recent study showed that cortactin displaces WASp from Arp2/3 complex specifically in the presence of actin filaments (Uruno *et al.* 2003). Thus, cortactin may help recycle WASp after nucleation has occurred, making WASp available for new rounds of nucleation and stabilizing the actin filament branch point created by the initial nucleation event (Weaver *et al.* 2002). In yeast, Las17/WASp and Pan1 show similar timing of appearance on newly forming cortical actin patches, whereas Myo3/Myo5 and Abp1 appear later in patch development (Kaksonen *et al.* 2003; Huckaba *et al.* 2004; Jonsdottir and Li 2004). Together, these studies suggest that different NPFs may act either in parallel or in series to control Arp2/3 complex activities.

To more clearly define the relationships among NPFs in *S. cerevisiae*, we tested all pairwise combinations of NPF mutants for genetic interactions. In addition, we crossed each NPF mutant to seven different conditional alleles of *arp2*. We then purified Arp2/3 complex from several of the *arp2* mutant strains and compared their ability to promote actin nucleation to determine the basis of their differential genetic interactions. Two distinct classes of *arp2* mutant activities were revealed: nucleation-impaired and unregulated or "leaky" nucleation (*i.e.*, promote actin assembly in the absence of NPFs). Our analyses of the nucleation-impaired mutants demonstrate the importance of barbed end actin nucleation by Arp2 for proper function of the Arp2/3 complex *in vitro* and *in vivo*. Differential genetic interactions with NPFs were observed for the two classes of *arp2* alleles. These and other data suggest that Las17, Pan1, and Myo3/Myo5 have distinct yet overlapping roles in promoting Arp2/3 complex-dependent actin nucleation *in vivo*, whereas Abp1 may attenuate the activities of the stronger NPFs.

MATERIALS AND METHODS

Yeast strains, plasmid constructions, and DNA manipulations: *S. cerevisiae* strains used in this study are listed in Table 1. Standard methods were employed for DNA manipulations, growth, and transformation of yeast (Guthrie and Fink 1991). For suppression analyses, *abp1*Δ *las17*Δ and *arp2 abp1*Δ double-mutant strains were transformed with a low-copy (CEN) plasmid expressing Abp1, pABP1 (Lila and Drubin 1997), or empty vector (pRS315), grown to saturation in selective media, and then plated in 10-fold serial dilutions on selective media and grown for 3 days at the indicated temperature. The pML9 vector (Longtine *et al.* 1998) was modified to include a TEV protease recognition site, generating pML9T. This vector was used to integrate a tag consisting of an in-frame TEV protease recognition site followed by three copies of the hemagglutin (HA) epitope at the C termini of the *ARP3* and *ARC18* genes, producing BGY623 (*ARP3::TEV-3HA::HIS3mX6*) and BGY694 (*ARC18::TEV-3HA::HIS3mX6*). pML9T was used by the Drubin lab to produce BGY741 (*ARC15::TEV-3HA::HIS3mX6*), a strain that they provided for us.

Antibodies and immunoblotting: Rabbit polyclonal antibody against yeast tubulin was a gift from Frank Solomon (Massachusetts Institute of Technology) and was used to demonstrate equal protein loading on immunoblots (*e.g.*, Figure 2B). Rabbit polyclonal antibody against Arp2 (Moreau *et al.* 1996) was a gift from Barbara Winsor (Centre National de Recherche Scientifique, Université Louis Pasteur, Strasbourg, France). Chicken polyclonal antibodies were raised against *S. cerevisiae* actin and the VCA fragment of Las17 (Aves; Tigard, OR). Antibodies were used for immunoblotting at 1:20,000 (actin), 1:4,000 (VCA), 1:20,000 (tubulin), and 1:1000 (Arp2). HRP-conjugated secondary antibodies were used at 1:10,000, and blots were developed with ECL (AP Biotech).

Cell-free actin assembly assay: Frozen yeast cells were lysed by mechanical shearing in liquid nitrogen (Goode 2002). HE buffer (20 mm HEPES, pH 7.5, 1 mm EDTA) and protease inhibitors (final concentration of 0.5 μg/ml each of antipain, leupeptin, pepstatin A, chymostatin, aprotinin, and 1 mm PMSF) were then added to a 1:1 ratio (v/w). The thawed lysates were clarified by centrifugation at 4°, 20 min at 80,000 rpm in a TLA100.3 rotor (Beckman, Fullerton, CA). The resulting high-speed supernatants (HSS) were normalized after measuring protein concentration by two methods: Bradford assay and comparison of samples on Coomassie-stained gels. Normalized HSS fractions were incubated at 4° for 2 hr to allow actin to assemble. Actin in polymer was pelleted by centrifuging the reactions at 80,000 rpm for 5 min in a TLA100 rotor at 4°. Supernatants and pellets were fractionated on SDS-PAGE gels, immunoblotted with actin antibodies. Signals were quantified by scanning densitometry.

Protein purification: Arp2/3 complex was isolated from wild-type and *arp2* mutant strains with TEV-HA epitope tags integrated at the C terminus of the gene encoding the Arp3, Arc18/ARPC3, or Arc15/ARPC5 subunit. For a single preparation, 4 liters of yeast culture in YPD were grown to OD_{600} = 0.8, washed, resuspended in a 3:1 ratio (w/v) of cell pellet to H_2O, and frozen in liquid nitrogen. Cells were lysed as above, and then the frozen cell powder was thawed in a 1:1 (w/v) ratio of room temperature HEK buffer (20 mm HEPES, pH 7.5, 1 mm EDTA, 50 mm KCl) and protease inhibitors (as above). Lysate (15 ml) was centrifuged for 20 min at 80,000 rpm (260,000 × *g*) in a TLA100.3 rotor. The supernatant was incubated with 100 μl of protein A-CL4B (AP Biotech) beads bound to anti-HA antibodies (HA.11; Covance) (Goode *et al.* 2001). After 2 hr of incubation, the beads were washed three times with HEK (1.5 ml), once with 1.5 ml HEKT (20 mm HEPES, pH 7.5, 1 mm EDTA, 50 mm KCl, 0.5% v/v Triton X-100), two times with 1.5 ml HEK_{500} (20 mm HEPES, pH 7.5, 1 mm EDTA, 500 mm KCl), and once with 1.5 ml HEK. Beads were then resuspended in 100 μl of HEK to create a 1:1 bead slurry. Two units of recombinant TEV protease (Invitrogen) were added, proteins were incubated for 1 hr at room temperature, and then two more units of TEV protease were added and the proteins were incubated for an additional hour. The supernatant was removed from the beads by low-speed

TABLE 1

***S. cerevisiae* strains used in this study**

Strain	Genotype (all S288c background)	Source
BGY134	*MAT*α, *ade2-1, his3,11-15, leu2-3,112, trp1-1, ura3-52, ARP2::URA3*	Madania *et al.* (1999)
BGY136	*MAT*α, *ade2-1, his3,11-15, leu2-3,112, trp1-1, ura3-52, arp2-1::URA3*	Madania *et al.* (1999)
BGY137	*MAT*α, *ade2-1, his3,11-15, leu2-3,112, trp1-1, ura3-52, arp2-2::URA3*	Madania *et al.* (1999)
BGY138	*MAT*α, *ade2-1, his3,11-15, leu2-3,112, trp1-1, ura3-52, arp2-3::URA3*	Madania *et al.* (1999)
BGY139	*MAT*α, *ade2-1, his3,11-15, leu2-3,112, trp1-1, ura3-52, arp2-4::URA3*	Madania *et al.* (1999)
BGY140	*MAT*α, *ade2-1, his3,11-15, leu2-3,112, trp1-1, ura3-52, arp2-5::URA3*	Madania *et al.* (1999)
BGY141	*MAT*α, *ade2-1, his3,11-15, leu2-3,112, trp1-1, ura3-52, arp2-6::URA3*	Madania *et al.* (1999)
BGY142	*MAT*α, *ade2-1, his3,11-15, leu2-3,112, trp1-1, ura3-52, arp2-7::URA3*	Madania *et al.* (1999)
BGY623	*MAT***a**, *ade2-1, his3,11-15, leu2-3,112, ura3-52, ARP3-TEV3HA::HIS3mX6*	This study
BGY694	*MAT*α, *ade2-1, his3,11-15, leu2-3,112, trp1-1, ura3-52 ARC18-TEV3HA::HIS3mX6*	Rodal *et al.* (2005b)
BGY741	*MAT*α, *ade2-1, his3,11-15, leu2-3,112, trp1-1, ura3-52, ARC15-TEV3HA::HIS3mX6*	Drubin lab
BGY807	*MAT***a**, *his3,11-15, leu2-3,112,TRP1, LYS2, ura3-52, arc35*Δ*::KANmX, LEU2::arc35-5::LEU2*	Rodal *et al.* (2005a)
BGY809	*MAT***a**, *his3,11-15, leu2-3,112,TRP1, LYS2, ura3-52, arc35*Δ*::KANmX, LEU2::arc35-6::LEU2*	Rodal *et al.* (2005a)
BGY915	*MAT*α, *ade2-1, his3,11-15, leu2-3,112, trp1-1, ura3-52, ARP2::URA3, ARC18-TEV3HA::HISmX6*	This study
BGY916	*MAT*α, *ade2-1, his3,11-15, leu2-3,112, trp1-1, ura3-52, arp2-2::URA3, ARC18-TEV3HA::HISmX6*	This study
BGY917	*MAT*α, *ade2-1, his3,11-15, leu2-3,112, trp1-1, ura3-52, arp2-5::URA3, ARC18-TEV3HA::HISmX6*	This study
BGY918	*MAT*α, *ade2-1, his3,11-15, leu2-3,112, trp1-1, ura3-52, arp2-6::URA3, ARC18-TEV3HA::HISmX6*	This study
BGY919	*MAT*α, *ade2-1, his3,11-15, leu2-3,112, trp1-1, ura3-52, arp2-7::URA3, ARC18-TEV3HA::HISmX6*	This study
BGY920	*MAT*α, *ade2-1, his3,11-15, leu2-3,112, trp1-1, ura3-52, ARP2::URA3, ARC15-TEV3HA::HISmX6*	This study
BGY921	*MAT*α, *ade2-1, his3,11-15, leu2-3,112, trp1-1, ura3-52, arp2-1::URA3, ARC15-TEV3HA::HISmX6*	This study
BGY924	*MAT*α, *his3*Δ*200, leu2-3,112, lys2-801(oc), ura3-52, pan1-101::LEU2*	This study
DDY2859	*MAT***a**, *his3*Δ*200, leu2-3,112, lys2-801(oc), ura3-52, PAN1::LEU2*	Drubin lab
DDY2860	*MAT***a**, *his3*Δ*200, leu2-3,112, lys2-801(oc), ura3-52, pan1-101::LEU2*	Drubin lab
HA31-9C	*MAT***a**, *ade2-201, can1-100, his3,11-15, leu2-3,112, trp1-1(am), ura3-52, myo3*Δ*::HIS3, myo5*Δ*::TRP1*	Anderson *et al.* (1998)
MDY6-1B	*MAT*α, *ade1-101, his3*Δ*200, leu2-3,112, lys2-801(oc), trp1-1, ura3-52, las17*Δ*::URA3*	Drubin lab

Strains BGY741, DDY2859, DDY2860, and MDY6-1B were provided by the Drubin laboratory.

centrifugation, aliquoted, and flash-frozen in liquid nitrogen. rTEV has no effect on Arp2/3 complex-mediated actin polymerization (Rodal *et al.* 2003).

Rabbit skeletal muscle actin (Pollard 1984), yeast actin (Goode 2002), full-length Las17 (Rodal *et al.* 2003), and Abp1-AN*C* (Goode *et al.* 2001) were purified as described. Wild- type Abp1 and Abp1ΔADFH were isolated from BJ2168 (Jones 2002) transformed with pGalABP1 or pGalABP1Δ ADFH (Quintero-Monzon *et al.* 2005). High-level expression was induced with galactose as described (Rodal *et al.* 2002). A high-speed supernatant was generated as above using HEK buffer and applied to a HiTrap Q FF 5-ml anion exchange column (AP Biotech). Proteins were eluted with a linear gradient of KCl (0.2–0.6 m) in HEK buffer and 5% glycerol. Peak fractions were pooled, diluted to 0.1 m KCl using HE buffer, and loaded onto a Mono Q (5/5) column. Proteins were eluted with a linear gradient of KCl (0.25–0.60 m) in HEK buffer plus 5% glycerol. Peak fractions were concentrated to 300 μl and applied to a Superose-12 (10/30) gel filtration column equilibrated in HEK buffer. Peak fractions were concentrated to 15–75 μm, aliquoted, and flash frozen in liquid N_2.

Actin assembly kinetics: Rabbit skeletal muscle actin was labeled with pyrenyliodoacetamide as described (Pollard 1984; Higgs *et al.* 1999). Actin monomers were prepared by gel filtration using a Sephacryl S-200 column equilibrated in G-buffer (10 mm Tris, pH 8.0, 0.2 mm ATP, 0.2 mm $CaCl_2$, and 0.2 mm DTT). Actin filament assembly assays were performed as described (Xu *et al.* 2004). Briefly, gel-filtered actin monomers (final concentration 3 μm, 5% pyrene labeled) were mixed with exchange buffer (10 mm EGTA, 1 mm $MgCl_2$) for 2 min (Kovar *et al.* 2003) and then mixed with 10 μl of HEK buffer or proteins in HEK buffer. This mixture was added immediately to 3 μl of 20× initiation mix (40 mm $MgCl_2$, 10 mm ATP, 1 m KCl) to initiate actin assembly. Pyrene fluorescence was monitored at excitation 365 nm and emission 407 nm in a fluorescence spectrophotometer (Photon Technology International) at 25°. The rate of polymerization was calculated from the slopes of assembly curves at ~20–50% polymerization. The number of free barbed ends was calculated as described (Pollard 1986).

RESULTS

Genetic relationships among yeast nucleation-promoting factors: To begin to dissect the *in vivo* relationships among *S. cerevisiae* NPFs, we tested all pairwise genetic interactions among *las17*Δ, *pan1-101*, *myo3*Δ*myo5*Δ, and *abp1*Δ mutations. Directed crosses were performed between haploid strains bearing these mutations. Diploids were selected, sporulated, and the resulting haploid progeny (wild type, single mutants, and double mutants) were compared for growth at 25°, 30°, 34°, and 37°. The resulting genetic interactions are diagrammed in Figure 1A. Combining *las17*Δ with *myo3*Δ*myo5*Δ was lethal at all temperatures, consistent with previous studies (Evangelista *et al.* 2000; Lechler *et al.* 2000). In contrast, *pan1-101*, which carries a mutation in its acidic motif required for Arp2/3 complex activation, had a genetic interaction with *las17*Δ, but not *myo3*Δ*myo5*Δ. These data suggest that Las17 and type I

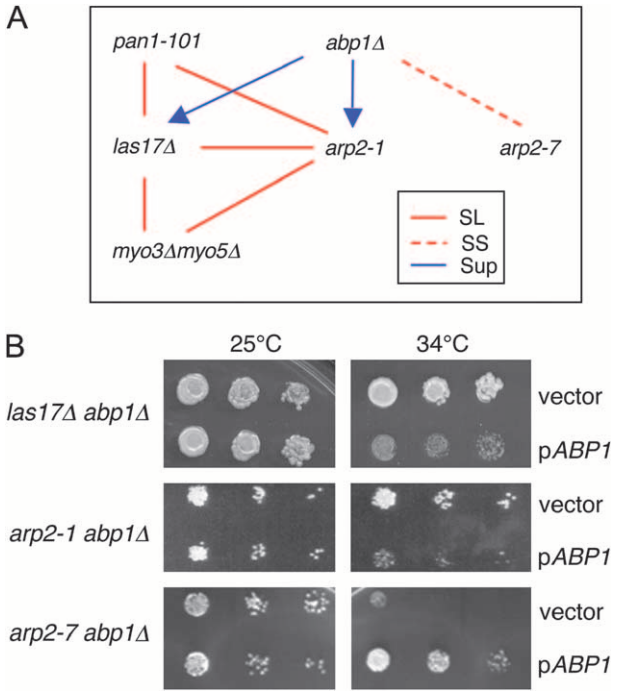

Figure 1.—Genetic interactions among nucleation-promoting factor mutants and *arp2* alleles. (A) Diagram of genetic relationships. Six haploid strains bearing *las17*Δ, *abp1*Δ, *myo3*Δ *myo5*Δ, *pan1-101*, *arp2-1*, and *arp2-7* mutations were crossed in all pairwise combinations to test genetic interactions. The data for *arp2* alleles are summarized in Table 2. The absence of a line indicates that no interaction was detected. SL, synthetic lethal; SS, synthetic sick; SUP, suppression. The direction of the arrow indicates direction of suppression. Thus, the growth defects of both *arp2-1* and *las17*Δ strains are partially suppressed by *abp1*Δ. (B) Differential genetic interactions of *abp1*Δ with *las17*Δ, *arp2-1*, and *arp2-7* mutations. Haploid *abp*Δ *las17*Δ, *abp1*Δ *arp2-1*, and *abp1*Δ *arp2-7* strains were transformed with a pABP1 CEN expression plasmid (Lila and Drubin 1997) or empty vector, plated on selective media, and grown at 25° and 34°.

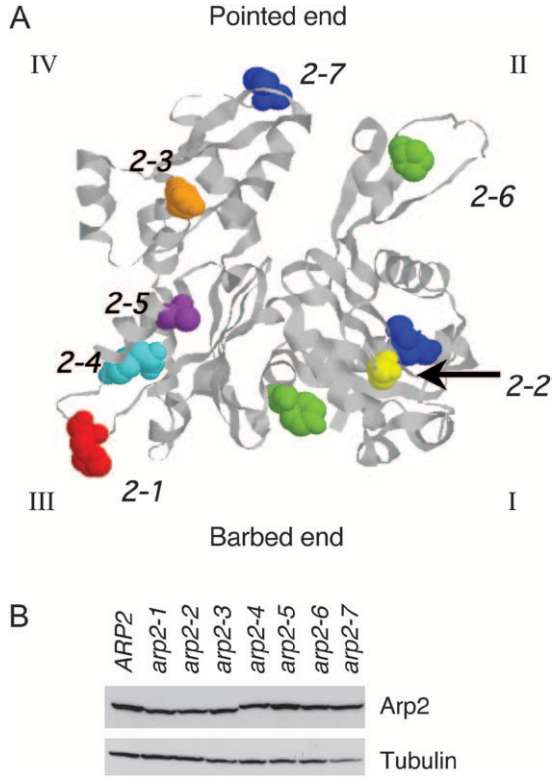

Figure 2.—Positions of residues mutated in *arp2* alleles and Arp2 expression levels in the mutant strains. (A) The residues mutated in each *arp2* allele (Table 1) are highlighted on the crystal structure of rabbit skeletal muscle actin (1ATN). The crystal structure of Arp2 is not shown because only half of its structure is solved (Robinson *et al.* 2001). The four subdomains (I, II, III, and IV) are indicated, and the Arp2-specific loop in subdomain III was inserted from a crystallized portion of Arp2 (1K8K). The specific residues mutated in each allele are shown in space-fill and color-coded: *arp2-1* (red), *arp2-2* (yellow), *arp2-3* (orange), *arp2-4* (cyan), *arp2-5* (purple), *arp2-6* (green), and *arp2-7* (blue). (B) Arp2 protein levels were compared in wild-type and *arp2* mutant cells grown to log phase by immunoblotting total cell extracts with Arp2 antibodies. The same samples were immunoblotted with tubulin antibodies as a loading control. Although some lanes on the tubulin blot show a lower signal (*e.g.*, *arp2-7*), repeated experiments demonstrated that variation was due to inefficient transfer of some lanes and that tubulin and Arp2 levels are similar in whole-cell extracts from these strains (not shown).

myosins have distinct yet overlapping functions *in vivo*, consistent with the partial overlap in their temporal patterns of association with actin patches (Jonsdottir and Li 2004 and see discussion).

Interestingly, combining *abp1*Δ with other NPF mutations (*las17*Δ, *pan1-101*, and *myo3*Δ*myo5*Δ) did not cause any synthetic phenotypes. Instead, *abp1*Δ suppressed the growth defects of *las17*Δ (Figure 1A), improving growth at 25° and permitting growth at the restrictive temperature (34°), which was never observed for *las17*Δ cells. Suppression also was observed independently in isogenic strains by comparing the growth of a *las17*Δ *abp1*Δ strain transformed with either a low-copy *ABP1* expression plasmid or empty vector (Figure 1B). Thus, in two different assays, *las17*Δ *abp1*Δ cells grew more robustly than *las17*Δ cells. These data point to a unique function for Abp1, possibly antagonistic to other NPFs.

Genetic interactions among nucleation-promoting factors and *arp2* alleles: We reasoned that we may be able to separate further the roles of NPFs using a collection of mutant alleles in *arp2*, for which differential genetic interactions with *las17*Δ were reported previously (Madania *et al.* 1999). The seven conditional *arp2* alleles were generated by random mutagenesis, and each allele contains either one or two single-point mutations (Moreau *et al.* 1996). The positions of the residues mutated in each allele are modeled on the crystal structure of actin to highlight their approximate positions in Arp2 (Figure 2A). We found that all seven *arp2* alleles have defects in both actin organization and endocytosis (not shown), consistent with the original study (Moreau *et al.* 1996). It also had been reported that all of the alleles except for *arp2-7* are lethal in

TABLE 2

Genetic interactions between *arp2* alleles and nucleation-promoting factors

Allele	Mutation(s)[a]	*LAS17* OE[b]	*las17*Δ[b]	*abp1*Δ	*myo3*Δ, *myo5*Δ	*pan1-101*
ARP2		NE	NE	NE	NE	NE
arp2-1	H330L	Sup	SL	Sup	SL	NE
arp2-2	G19D	Sup	SL	Sup	SL	Sup
arp2-3	E256K	NE	SL	NE	NE	SS
arp2-4	L280P	NE	SL	SL	NE	Sup
arp2-5	L316S	NE	SL	SS	NE	SS
arp2-6	G35S, Y144N	NE	SL	SS	NE	NE
arp2-7	F127S, F203Y	NE	NE	SS	NE	NE

NE, no effect; SL, synthetic lethal; SS, synthetic sick; Sup, suppression (growth at 37° for double mutants, which was never observed for single mutants).

[a] Data from Moreau *et al.* (1996).

[b] Data from Madania *et al.* (1999).

combination with *las17*Δ at 25°, and the temperature-sensitive growth defects of *arp2-1* and *arp2-2* are suppressed by overexpression of Las17 (Madania *et al.* 1999). This suggested that the alleles might provide excellent tools for separating NPF functions.

We crossed each NPF mutant strain (*las17*Δ, *abp1*Δ, *myo3*Δ *myo5*Δ, and *pan1-101*) to strains expressing each temperature-sensitive *arp2* allele (*arp2-1* through *arp2-7*). The genetic interactions we observed between *arp2* alleles and *las17*Δ are consistent with previous work (Madania *et al.* 1999). Additionally, we identified new genetic interactions between *arp2* alleles and *myo3*Δ*myo5*Δ, *pan1-101*, and *abp1*Δ (Table 2).

Two alleles, *arp2-1* and *arp2-2*, were synthetic lethal with *las17*Δ and *myo3*Δ*myo5*Δ. These data support the genetic grouping of *arp2-1* and *arp2-2* and are consistent with the observation that *LAS17* and *MYO3/MYO5* share overlapping genetic functions (above). In contrast, *arp2-7* showed no genetic interactions with *las17*Δ or *myo3*Δ *myo5*Δ and was synthetic sick with *abp1*Δ. We demonstrated independently the specificity of this genetic interaction between *arp2-7* and *abp1*Δ in an isogenic background by comparing the growth of *arp2-1 abp1*Δ and *arp2-7 abp1*Δ strains transformed with an *ABP1* plasmid or empty vector (Figure 1B). The temperature sensitivity caused by *arp2-1* was rescued by *abp1*Δ. Together, these data place *arp2-7* in a distinct genetic category from *arp2-1* and *arp2-2*. The remaining *arp2* alleles (*arp2-3*, *arp2-4*, *arp2-5*, and *arp2-6*) showed complex patterns of genetic interactions that were difficult to interpret. This is likely to result from these alleles having multiple defects in Arp2/3 complex activities and functions. Therefore, we focused primarily on *arp2-1*, *arp2-2*, and *arp2-7* in our further analyses.

The patterns of genetic interactions observed between *arp2* alleles and NPF mutants neither correlate with differences in the severity of growth defects caused by the mutations (not shown) nor result from differences in Arp2 expression levels (Figure 2B). The specificity of the genetic interactions prompted us to investigate the underlying biochemical basis of the *arp2* defects.

Isolation of wild-type and *arp2* mutant Arp2/3 complexes: For a fair comparison of their activities, it was important to isolate Arp2/3 complex from wild-type, *arp2-1*, *arp2-2*, and *arp2-7* strains by the same method. Initially, we used our previously described method for isolating wild-type yeast Arp2/3 complex, which relies on an initial step of reconstituting actin assembly in clarified yeast cell lysates at 4° (Goode 2002). This assay cannot be performed at higher temperatures due to proteolysis effects. Recently, we determined that actin assembly in this assay requires Arp2/3 complex and Las17, but not other NPFs (A. Goodman, J. L. D'Agostino and B. L. Goode, unpublished results). Therefore, it stands to reason that actin assembly will fail in cell extracts from *arp2* mutants with severely compromised actin nucleation activity. As shown in Figure 3A, actin assembly failed in cell extracts from five of the seven *arp2* strains, despite the fact that they had comparable levels of both actin (Figure 3B) and Arp2 (Figure 2B). In particular, we noted that cell extracts from *arp2-1* and *arp2-2* strains failed to polymerize actin, whereas extracts from *arp2-7* cells polymerized actin like wild-type extracts. These data are consistent with the differential genetic interactions of these *arp2* alleles with *LAS17* and provided the first indication of key differences in the biochemical defects of *arp2-1* and *arp2-2* compared to *arp2-7*.

Since the cell extract method could not be used to isolate Arp2/3 complex from *arp2-1* and *arp2-2* strains, we developed an alternative strategy that employs an integrated C-terminal affinity tag on one subunit of the Arp2/3 complex. The tag consists of a TEV protease recognition site followed by three copies of the hemagglutin (HA) epitope, and importantly, it is removed from Arp2/3 complex during purification, leaving only a short remnant on one subunit (see materials and methods). Prior to its removal though, the tag partially compromises Arp2/3 complex function *in vivo*, as indicated by the partially impaired growth of tagged

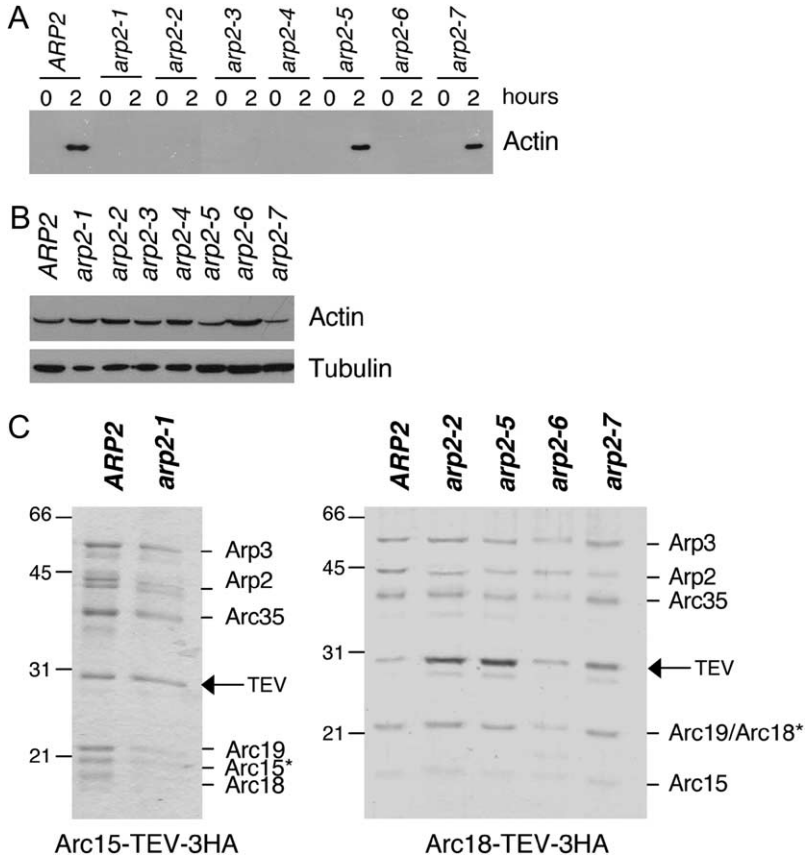

FIGURE 3.—Purification of Arp2/3 complex from wild-type and *arp2* mutant strains. (A) Clarified cell extracts isolated from wild-type and *arp2* strains were compared for their ability to nucleate actin assembly over time. Samples of reactions were removed at time zero and after 2 hr of incubation at 4° and centrifuged at 80,000 × *g* to pellet polymerized actin (GOODE 2002). Actin levels in the pellets were analyzed by SDS-PAGE and immunoblotting with actin antibodies; >50% of the cellular actin assembles in wild-type extracts (A. GOODMAN, J. L. D'AGOSTINO and B. L. GOODE, unpublished results). (B) Starting actin levels in the clarified extracts were compared by immunoblotting with actin antibodies. The same samples were immunoblotted with tubulin antibodies as a loading control. (C) Coomassie-stained gels of Arp2/3 complex isolated from wild-type (*ARP2*) and *arp2* strains. A TEV-3xHA affinity tag integrated at the C terminus of the Arc15/ARPC5 subunit was used to isolate Arp2/3 complex from wild-type and *arp2-1* strains. A similar tag on the Arc18/ARPC3 subunit was used to isolate Arp2/3 complex from wild-type, *arp2-2*, *arp2-5*, *arp2-6*, and *arp2-7* strains. A remnant of nine residues is left on the indicated subunit after TEV protease digestion, causing the aberrant migration of that subunit (*).

strains at higher temperatures and synthetic genetic interactions between tagged subunits and *arp2* alleles (Table 3). Tagging Arp2 in each of the seven *arp2* strains resulted in lethality, indicating that this single subunit cannot function properly if both mutated and tagged. However, other tagged subunits (Arp3, Arc18/ARPC3, and Arc15/ARPC5) were found to be viable in combination with specific *arp2* alleles: *arp2-1*, *arp2-2*, *arp2-5*, *arp2-6*, and *arp2-7* alleles. Thus, an Arc18/ARPC3 tag was used to isolate Arp2/3 complex from wild-type, *arp2-2*, *arp2-5*, *arp2-6*, and *arp2-7* strains, and an Arc15/ARPC5 tag was used to isolate Arp2/3 complex from wild-type and *arp2-1* strains (Figure 3C). All of the tagged subunits tested were synthetic lethal with *arp2-3* and *arp2-4* (Table 3), precluding the isolation of Arp2/3 complex from these strains.

Purified wild-type and *arp2* mutant Arp2/3 complexes are shown fractionated on SDS-PAGE gels (Figure 3C).

TABLE 3

Genetic interactions between *arp2* alleles and tagged subunits of the Arp2/3 complex

Allele	*ARP2-T-3xHA*	*ARP3-T-3xHA*	*ARC18-T-3xHA*	*ARC15-T-3xHA*
ARP2	Viable	Viable	Viable	Viable
arp2-1	SL	SL	SL	Viable[a]
arp2-2	SL	Viable[a]	Viable	Viable
arp2-3	SL	SL	SL	SL
arp2-4	SL	SL	SL	SL
arp2-5	SL	Viable	Viable	SL
arp2-6	SL	SL	Viable	SL
arp2-7	SL	Viable	Viable	SL

Each subunit has at its carboxyl terminus an integrated tag consisting of a TEV protease cleavage site followed by three copies of the HA epitope. All of the viable haploid strains are underlined, and unless otherwise noted, viable haploid strains grow at 25° in rich medium. SL, synthetic lethal.

[a] Viable at 25° when medium is supplemented with 0.9 M sorbitol.

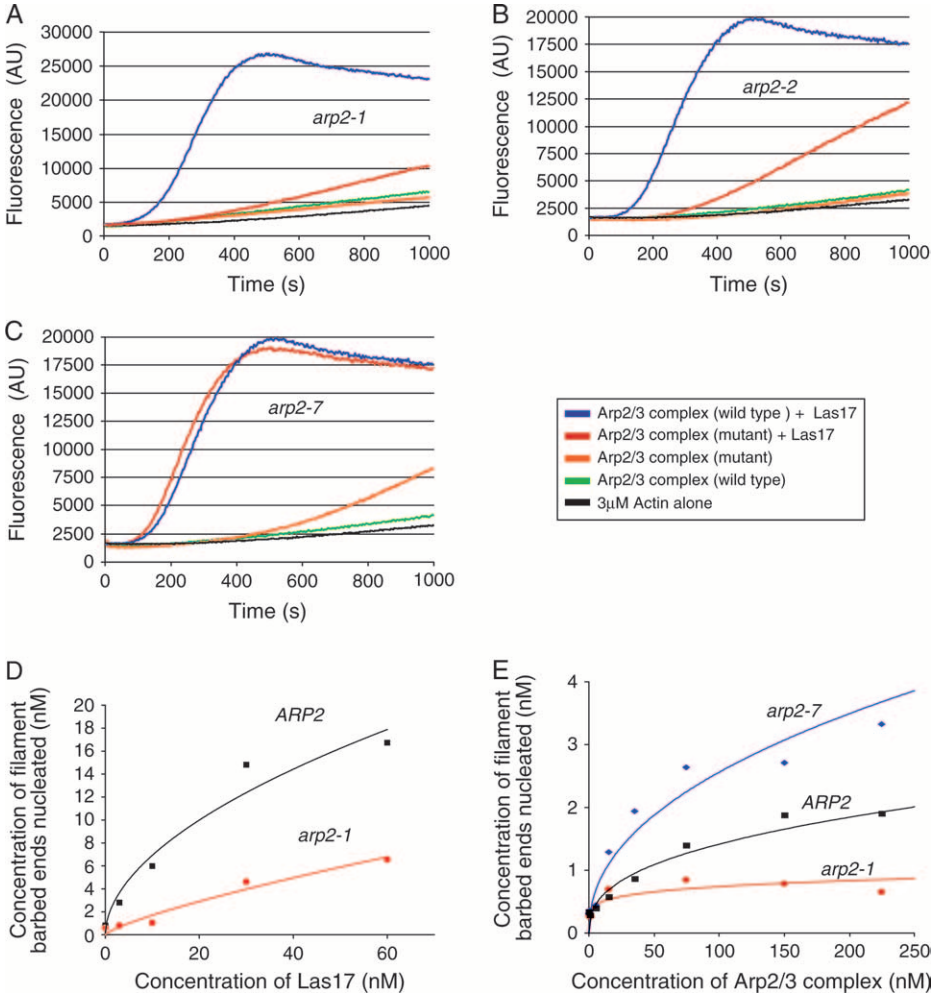

FIGURE 4.—Actin nucleation activities of Arp2/3 complexes isolated from wild-type and mutant *arp2* strains. (A–C) Assembly of monomeric actin (3 μM, 5% pyrene labeled) was compared in the presence and absence of 15 nM full-length Las17 and 15 nM wild type or *arp2-1* (A), *arp2-2* (B) or *arp2-7* (C) Arp2/3 complex. (D) Comparison of the actin nucleation activities of wild-type and *arp2-1* Arp2/3 complexes (15 nM) in the presence of variable concentrations of Las17. (E) Quantitative comparison of actin nucleation activities for wild-type, *arp2-1*, and *arp2-7* Arp2/3 complexes in the absence of Las17.

The positions of six of the seven subunits in the complex are labeled. Mass spectrometry analysis showed that the remaining subunit p40/ARPC1 is present (data not shown); however, this subunit in *S. cerevisiae* exhibits aberrant gel mobility (PAN *et al.* 2004). The remnant from the tag causes signature differences in the gel mobilities of Arc18/ARPC3 and Arc15/ARPC5 (asterisks, Figure 3C). However, the activity of wild-type Arp2/3 complex prepared using either tag (Arc18/ARPC3 or Arc15/ARPC5) was indistinguishable from tag-less wild-type Arp2/3 complex isolated by the extract method (not shown, and RODAL *et al.* 2003, 2005a). Further, we isolated *arp2-7* Arp2/3 complex separately using two different tagged subunits (Arc18/ARPC3 and Arp3) and found their actin nucleation activities to be indistinguishable.

Distinct biochemical defects in the activities of *arp2-1* and *arp2-7* Arp2/3 complexes: Next, we directly compared the actin nucleation capabilities of the wild-type and mutant *arp2* Arp2/3 complexes (Figure 4). The pyrene-actin assembly assay was used to monitor assembly kinetics of purified actin monomers (3 μM) in the presence of wild-type or mutant Arp2/3 complex (15 nM) with and without full-length Las17 (15 nM). As expected, wild-type, *arp2-1*, and *arp2-2* Arp2/3 complexes alone had little actin nucleation activity in the absence of Las17 (Figure 4, A and B). Addition of Las17 strongly stimulated wild-type Arp2/3 complex, but had minimal stimulatory effects on *arp2-1* and *arp2-2* Arp2/3 complexes, indicating that these mutations cause impaired actin nucleation. Given that *LAS17* (a strong NPF) was identified as a multicopy suppressor of *arp2-1* (MADANIA *et al.* 1999), we tested whether higher concentrations of Las17 could biochemically restore actin nucleation function to *arp2-1* mutant Arp2/3 complex. Therefore, we compared the nucleation activities of wild-type and *arp2-1* Arp2/3 complexes over a range of Las17 concentrations (3–60 nM). Addition of increasing Las17 concentrations increased the nucleation activity of *arp2-1* Arp2/3 complex in a dose-responsive manner (Figure 4D). These data offer a biochemical explanation for why overexpression of Las17 can suppress *arp2-1* defects *in vivo*. The biochemical defects of the purified *arp2-1* and *arp2-2* mutant Arp2/3 complexes are also consistent with the genetic interactions of these alleles with *LAS17* (Table 2) and with the failure of actin to assemble in cell extracts from *arp2-1* and *arp2-2* strains (Figure 3A). Importantly, the data also show that *arp2-1*

TABLE 4

Genetic interactions of *arp2* alleles with *arc35* alleles

Genotype	25°	30°	34°	37°	Genetic interaction
Haploid					
ARP2, ARC35	+++	+++	+++	+++	NA
arp2-1, ARC35	+++	++	+	−	NA
arp2-7, ARC35	+++	++	+	−	NA
ARP2, arc35-5	+++	+++	++	++	NA
ARP2, arc35-6	+++	+++	+++	+++	NA
arp2-1, arc35-5	++	++	−	−	NE/SS
arp2-7, arc35-5	−	−	−	−	SL
arp2-1, arc35-6	++	−	−	−	SS
arp2-7, arc35-6	+++	++	+	−	NE
Diploid					
ARP2/ARP2	+++	+++	+++	+++	NA
arp2-1/ARP2	+++	+++	+++	+++	Recessive
arp2-7/ARP2	+++	+++	+++	+++	Recessive
arp2-1/arp2-1	+++	++	+	−	NA
arp2-7/arp2-7	+++	++	+	−	NA
arp2-1/arp2-7	+++	++	+	−	NE

Relative growth of yeast strains is expressed as +++, wild type; ++, partially compromised; +, severely compromised; and −, no growth. NA, not applicable; NE, no effect; SL, synthetic lethal; SS, synthetic sick.

Arp2/3 complex is impaired for actin nucleation, even in the absence of Las17. This suggests that a primary defect of *arp2-1* is in directly nucleating actin, which is also consistent with the mutations in these alleles residing at the barbed end (Figure 2A).

In contrast to *arp2-1* and *arp2-2* mutants, *arp2-7* Arp2/3 complex was activated normally by Las17, with activity similar to wild-type Arp2/3 complex (Figure 4C). However, *arp2-7* Arp2/3 complex showed aberrantly high nucleation activity in the absence of Las17, suggesting that this allele causes unregulated (leaky) nucleation activity. To characterize this effect more carefully, we compared the nucleation activities of wild-type, *arp2-1*, and *arp2-7* Arp2/3 complexes alone, in the absence of Las17, over a range of Arp2/3 complex concentrations (Figure 4E). This confirmed that *arp2-7* Arp2/3 complex is auto-activated. We also note that *arp2-7* Arp2/3 complex is not overactive compared to wild-type Arp2/3 complex in the presence of Las17 (Figure 4C), suggesting that *arp2-7* is not a gain-of-function mutant (*i.e.*, it does not alter Arp2 to improve its efficiency in nucleating actin). This is also consistent with our *in vivo* data; we detected no defects in cell growth or actin organization in heterozygous *arp2-7* diploids (Table 4, and data not shown); thus, *arp2-7* behaves as a recessive allele. On the basis of these results, we hypothesize that *arp2-7* disrupts the normal auto-inhibition by Arp2/3 complex that minimizes nucleation in the absence of NPFs (see DISCUSSION). Below we refer to *arp2-1* and *arp2-7* as nucleation-impaired and constitutively active mutants, respectively.

Genetic relationships between constitutively active and nucleation-impaired Arp2/3 complex mutants: Recently, we reported that another Arp2/3 complex mutant (*arc35-5*), like *arp2-7*, is partially constitutively active for nucleation (RODAL *et al.* 2005a). *arc35-5* is a partially temperature-sensitive allele of *ARC35*, which encodes the p35/ARPC2 subunit of Arp2/3 complex. Both *arp2-7* and *arc35-5* have actin organization defects at 25° (depolarized patches) and impaired or arrested cell growth at 37° (not shown). This indicates that cells can tolerate partial levels of unregulated nucleation by Arp2/3 complex at lower temperatures. To test whether cells can tolerate potentially higher levels of auto-activation, we crossed the *arc35-5* and *arp2-7* haploid strains and control strains (Table 4). The results show that *arp2-7* is synthetic lethal specifically with *arc35-5*, but not *arc35-6*, an allele that is nucleation impaired (RODAL *et al.* 2005a). Although we observed a slight negative genetic interaction between *arp2-1* and *arc35-5*, this interaction was much less pronounced than the synthetic lethal interaction between the two constitutively active alleles *arp2-7* and *arc35-5*. Together, these data suggest that combining two constitutively active mutations within the same Arp2/3 complex causes additive or synergistic negative effects *in vivo*. Thus, cells cannot tolerate a high level of unregulated actin nucleation by Arp2/3 complex.

We also tested whether constitutively active alleles (*arp2-7* and *arc35-5*) might have the capacity to suppress nucleation-impaired alleles (*arp2-1* and *arc35-6*). In other words, we asked if rendering the Arp2/3 complex partially unregulated (leaky) could rescue *in vivo* defects in nucleation, and vice versa. To address this question, we tested suppression by two criteria: (1) combining mutations in haploid strains and (2) testing complementation in diploid strains that are homozygous and heterozygous for constitutively active and nucleation-impaired alleles. As shown in Table 4, in no case was the mutant phenotypes suppressed. Thus, constitutively active mutations cannot rescue nucleation-impaired mutations, and vice versa.

Abp1 attenuates the nucleation-promoting activity of Las17 in a dose-responsive manner: In light of the biochemical activities of *arp2-1* and *arp2-7*, the genetic data in Table 2 suggest that Las17, Pan1, and Myo3/Myo5 cooperate to promote actin assembly *in vivo*, whereas Abp1 may act to suppress actin assembly by other NPFs. Three observations support this view: (1) *abp1*Δ is synthetic sick with *arp2-7* (constitutively active) but suppresses *arp2-1* (nucleation impaired); (2) *las17*Δ has synthetic interactions with *arp2-1*, but not *arp2-7*; and (3) *abp1*Δ suppresses *las17*Δ. Further, the biochemical properties of Abp1 are consistent with such a role as an attenuator. Abp1 has a relatively high affinity for Arp2/3 complex and yet also has notably weak nucleation-promoting activity (GOODE *et al.*

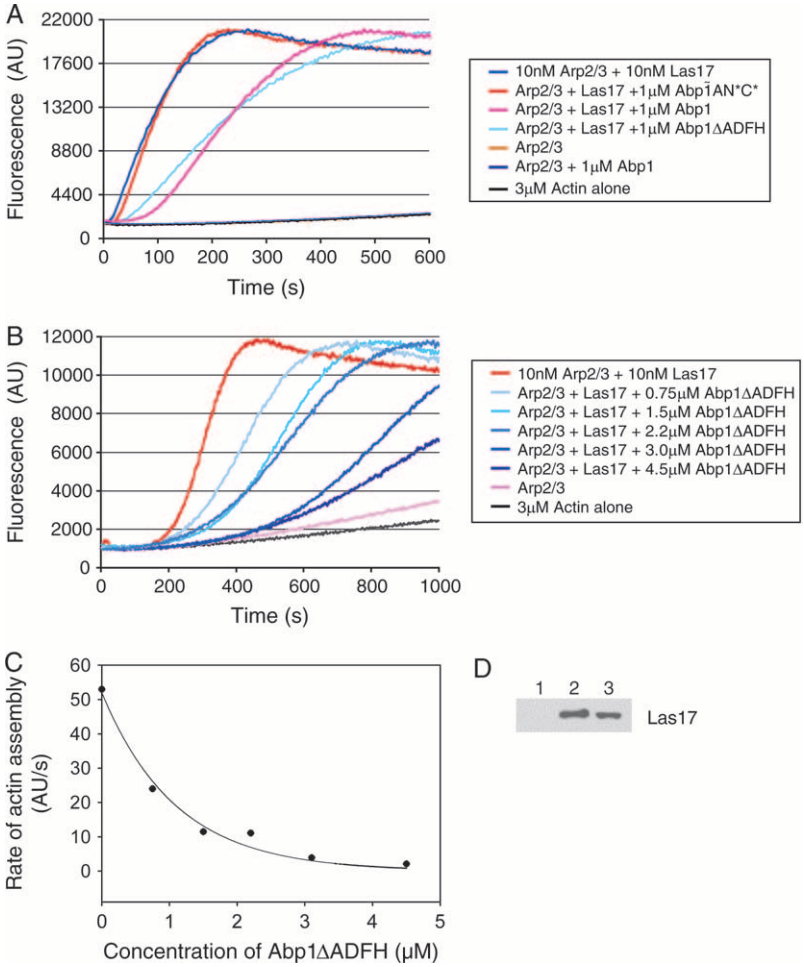

FIGURE 5.—Purified Abp1 attenuates the nucleation-promoting activity of Las17 on Arp2/3 complex in a dose-responsive manner. (A) Monomeric actin (3 μM, 5% pyrene-labeled) was polymerized in the presence of Arp2/3 complex (15 nM), Las17 (15 nM), and 1μM of each of the following proteins: full-length wild-type Abp1, Abp1ΔADFH, and Abp1-AN*C* (mutated to disrupt both of its acidic motifs). (B) Monomeric actin (as above) was polymerized in the presence of Arp2/3 complex (15 nM), Las17 (15 nM), and a range of concentrations of Abp1ΔADFH. (C) Graph showing the concentration-dependent effects of Abp1ΔADFH on rate of actin assembly induced by Las17 and Arp2/3 complex. (D) Association of Las17 (30 nM) with Arp2/3 complex (15 nM) is partially disrupted in the presence of excess Abp1 (2 μM). Beads coated with Arc18-HA-tagged Arp2/3 complex or control beads were incubated for 10 min with Las17 in the presence or absence of Abp1. Bead pellets were immunoblotted with anti-VCA antibody: Lane 1, control beads; lane 2, Arp2/3 beads without Abp1; lane 3, Arp2/3 beads with Abp1.

2001), especially compared to full-length Las17 (RODAL *et al.* 2003).

To test this model directly, we assayed the effects of purified Abp1 on Las17-Arp2/3 complex stimulated actin assembly *in vitro* (Figure 5). Abp1 has an N-terminal Actin Depolymerization Factor Homology (ADFH) domain that binds to actin filaments, whereas Las17 has a C-terminal WASp homology 2 (WH2) domain that associates with actin monomers. However, both Abp1 and Las17 associate with the Arp2/3 through conserved acidic motifs. Using an *in vitro* pyrene-actin assembly reaction, we tested the effects of adding Abp1 to reactions containing Las17 and Arp2/3 complex. Full-length wild-type Abp1 (1 μM) inhibited activation of Arp2/3 complex (15 nM) by Las17 (15 nM), but did not abolish it (Figure 5A). Abp1ΔADFH, which lacks nucleation-promoting activity, showed similar inhibitory effects, suggesting that inhibition may result from competition for Arp2/3 complex association by acidic motifs in Abp1 and Las17. Consistent with this hypothesis, a mutant of Abp1 (Abp1-AN*C*) that disrupts both of its Arp2/3-interacting acidic motifs (GOODE *et al.* 2001) failed to inhibit Las17 (Figure 5A). Thus, functional competition between Abp1 and Las17 is dependent on Abp1 acidic motifs.

To determine the half-maximal effect of Abp1 inhibition on Las17-Arp2/3, we repeated the assay over a range of Abp1 concentrations (0–4.5 μM) (Figure 5B). Abp1-ΔADFH was used for this determination because it inhibits Las17 as well as Abp1 but lacks nucleation-promoting activity, simplifying the interpretation of the results. As shown in Figure 5C, the half-maximal inhibition of Las17 was reached at 1 μM Abp1-ΔADFH. This demonstrates that Abp1 does in fact attenuate the activity of stronger NPFs in a dose-responsive manner. Although strong inhibition required significantly higher levels of Abp1 compared to Las17, we note that Abp1 is ≥10-fold more abundant *in vivo* than Las17 (A. GOODMAN, J. L. D'AGOSTINO and B. L. GOODE, unpublished results). Further, full-length Las17 has higher affinity than Abp1 for Arp2/3 complex (J. L. D'AGOSTINO, unpublished observations).

We next tested whether the functional competition between Abp1 and Las17 results from Abp1 displacement of Las17 from Arp2/3 complex. We measured direct binding of purified Las17 to Arp2/3 complex (15 nM Arp2/3 complex and 30 nM Las17, similar concentrations to those used in the functional assays above) in the presence and absence of excess Abp1 (2 μM). Partial displacement was observed (Figure 5D), consistent with

the partial functional competition at this concentration of Abp1 (Figure 5B). From these data, we propose that Abp1 interacts with Arp2/3 complex via its acidic domains, which disrupts important functional interactions between the acidic domain of Las17 and Arp2/3 complex. While this is sufficient to disrupt Las17 functional activation of Arp2/3 complex, it may or may not be sufficient to completely displace Las17 (physically) from Arp2/3 complex.

DISCUSSION

Las17, Pan1, and Myo3/Myo5 have overlapping roles in promoting Arp2/3 complex-dependent actin assembly *in vivo*: All of our genetic and biochemical data collectively suggest that Las17, Pan1, and Myo3/Myo5 cooperate *in vivo* to promote Arp2/3 complex-mediated actin assembly. This is demonstrated by their overlapping yet specific patterns of synthetic lethal interactions with each other and with *arp2* alleles that we found are biochemically impaired in actin nucleation. Cortical actin patch nucleation *in vivo* requires the Arp2/3 complex (Winter *et al.* 1999). However, our data show that only specific pairs of mutations among Las17, Pan1, and Myo3/Myo5 are synthetic lethal, suggesting that the Arp2/3 complex-stimulating activity of no single NPF is required *in vivo*. Instead, each NPF makes a specific and important contribution to the complex process of patch development/endocytosis, and these events involve the combined, partially redundant nucleation-promoting activities of multiple NPFs.

What might the overlapping physiological roles of NPFs be in these events? Until recently, it was unclear whether yeast NPFs acted in parallel or series. However, recent studies using dual-label imaging in live cells have shown that actin patches are the sites of endocytic internalization and mature in defined stages, marked by the arrival and departure of specific NPFs (Kaksonen *et al.* 2003; Huckaba *et al.* 2004; Jonsdottir and Li 2004). This allows us to put the genetic data obtained here into the context of cell function.

Las17 and Pan1 are present at early stages in the development of cortical actin patches (Kaksonen *et al.* 2003). Las17 is thought to play a central role in initiating Arp2/3-mediated actin assembly at patches on the basis of its potent nucleation-promoting activity *in vitro* (Rodal *et al.* 2003) and its severe loss-of-function phenotypes *in vivo* (Li 1997). Our genetic data suggest that Las17 and Pan1 may cooperate to activate Arp2/3 complex-mediated actin assembly, perhaps at this stage, which agrees with other recent reports (Toshima *et al.* 2005). Subsequently, Myo3/Myo5, Abp1, and Arp2/3 complex arrive at patches (Kaksonen *et al.* 2003; Jonsdottir and Li 2004). Myo3/Myo5 persists for a short window of time, during which it may promote membrane fission and endosome/patch internalization. We show that Las17 and Myo3/Myo5 are synthetic lethal, in agreement with previous studies (Evangelista *et al.* 2000; Lechler *et al.* 2000), suggesting that their functions may be overlapping at this stage in endocytosis. After scission, Pan1, Abp1, and Arp2/3 complex remain on patches as they begin to move inward rapidly, eventually to fuse with endosomal sorting compartments, whereas Las17 is left behind at the cell cortex (Kaksonen *et al.* 2003; Huckaba *et al.* 2004). These observations combined with our genetic data suggest that NPFs each have specialized yet intertwined roles in patch development. Specifically, our data suggest a role for Abp1 as an antagonist to other NPFs, possibly during scission, discussed below.

The studies above suggest that NPFs act both in parallel and in series during patch development. Assessment of the specific roles of each NPF requires consideration of which NPFs function together in physical complexes. Las17 and Myo3/Myo5 associate in cell extracts, and both proteins interact directly with Vrp1, which may link them (Evangelista *et al.* 2000). In addition, the SH3 domain-containing protein Sla1 associates with three different NPFs: Las17 (Li 1997; Rodal *et al.* 2003), Pan1 (Tang *et al.* 2000), and Abp1 (Gourlay *et al.* 2003). Thus, all four NPFs have the potential to be linked physically *in vivo*. Given their temporally distinct localization patterns to actin patches, it is likely that the complexes formed among NPFs change composition throughout patch development. This paints a complex picture of NPF coordination *in vivo*, and future deciphering of these events will likely require sophisticated microscopy approaches and biochemical tests in purified mixtures and/or cell-free extracts.

Abp1 performs a unique function as an NPF *in vivo*: The initial identification and characterization of Abp1 as an NPF (Goode *et al.* 2001) left two key questions open concerning its function: (1) Why does Abp1 bind to actin filaments and not monomers? and (2) Why does Abp1 have two acidic (A) motifs and tightly associate with Arp2/3 complex through gel filtration, yet have only weak nucleation-promoting activity compared to other NPFs? This latter point took on particular meaning after purified full-length Las17 was shown to have extremely potent and strong nucleation-promoting activity, over 2 orders of magnitude stronger than that of Abp1 (Rodal *et al.* 2003). The data presented here offer new insights into these questions surrounding Abp1 function.

Collectively, our data raise the possibility that Abp1 suppresses the activity of other NPFs. The primary observation leading to this model is that *abp1*Δ suppresses the growth defects of both *las17*Δ and *arp2-1*, mutations that impair Arp2/3 complex-mediated actin nucleation. Given that *las17*Δ creates a background in which cell viability depends on Pan1 and Myo3/Myo5 functions, Abp1 may antagonize one or both of these NPFs. Having two acidic domains may enable Abp1 to compete more effectively with other NPFs for functional

association with Arp2/3 complex. This could help recycle stronger NPFs after nucleation events and possibly stabilize filament branch points. Alternatively, this could serve as a competition mechanism that helps balance out NPF activities in a spatially and/or temporally controlled manner. Analogously, it has been shown that cortactin displaces WASp after nucleation has occurred (Uruno *et al.* 2003) and stabilizes Arp2/3-generated actin filament branch points (Weaver *et al.* 2002). Abp1 (and by analogy cortactin) also might function to attenuate stronger NPFs *in vivo*. The lack of an actin monomer-binding domain in Abp1 and cortactin likely explains why these two proteins have weak nucleation-promoting activities to begin with. These properties make them well suited for serving as attenuators of stronger NPFs. Conceptually this is similar to the expression of truncated (dummy) growth factor receptors to temper receptor responses to signals at the cell periphery.

What specific role might Abp1 play in patch development? Our data do not directly address this question but raise possibilities. Given the late arrival of Abp1 and Myo3/Myo5 at patches and our genetic results, it is tempting to speculate that Abp1 might attenuate Myo3/Myo5 function, thereby fine-tuning fission events preceding rapid patch movement inward from the cell cortex. This model is also consistent with *ABP1* being essential for endocytosis in specific *sla2* mutant backgrounds (Wesp *et al.* 1997) and *SLA2* being required for endocytic scission (Kaksonen *et al.* 2003; Rodal *et al.* 2005b).

Contributions of Arp2 to barbed end nucleation and auto-inactivation of Arp2/3 complex: Our biochemical data on *arp2* mutants make three important contributions to our understanding of Arp2/3 complex mechanism: (1) They provide the first experimental evidence for barbed end nucleation by Arp2 and/or Arp3 subunits, (2) they demonstrate the importance of barbed end nucleation by Arp2 *in vivo*, and (3) they offer insights into the mechanism by which Arp2/3 complex is maintained in an inactive state in the absence of NPFs. All current models for Arp2/3 complex function are predicated on the assumption that the barbed ends of Arp2 and Arp3 nucleate actin polymerization (Kelleher *et al.* 1995; Robinson *et al.* 2001; Beltzner and Pollard 2004). However, direct experimental data supporting this mechanism have been lacking. This fundamental model is based primarily on the high degree of sequence homology and structural similarity exhibited among Arp2, Arp3, and actin. Here, we found that two mutations located at the barbed end of Arp2 (*arp2-1* and *arp2-2*) are severely impaired for actin nucleation *in vitro*, providing direct experimental evidence for barbed end nucleation by Arp2/3 complex. Further, since these mutations cause strong defects in cell growth, actin organization, and endocytosis, this means that barbed end nucleation by Arp2/3 complex is critical *in vivo*.

The residue mutated in *arp2-1* (H330L) resides in a loop located at the barbed end (Figure 2A) that is predicted to contact the second actin subunit of the nucleated actin filament (Beltzner and Pollard 2004). This loop, which is divergent from actin, may provide specialized contacts between Arp2 and actin not found in actin-actin interactions, possibly to help stabilize association of the first actin subunits during nucleation. The residue mutated in *arp2-2* (G19D) resides in subdomain I at the barbed end. This residue is not solvent exposed, and therefore, the mutation likely disrupts barbed end nucleation by changing the conformation in subdomain I to weaken surface contacts between Arp2 and actin. Since both alleles (*arp2-1* and *arp2-2*) cause actin organizational defects *in vivo* and show genetic interactions with NPF mutants, this demonstrates that barbed end nucleation by Arp2/3 complex is critical *in vivo*. Further, these two alleles of *arp2* are suppressed by overexpression of Las17 *in vivo* (Madania *et al.* 1999), suggesting that their nucleation defects can be rescued in part by overproducing a strong NPF. This is consistent with our biochemical data showing that elevated concentrations of purified Las17 restore nucleation activity to *arp2-1* Arp2/3 complex (Figure 4D).

Our data also provide insights into how Arp2/3 complex is maintained in an inactive state, poised for activation by NPFs. In the crystal structure of Arp2/3 complex (NPFs absent), Arp2 and Arp3 are well separated (Robinson *et al.* 2001), and when NPFs are added, major structural rearrangements bring Arp2 and Arp3 closer to nucleate actin (Goley *et al.* 2004; Rodal *et al.* 2005a). Until such activation, what keeps Arp2 and Arp3 spatially separated? A recent study predicts that the specific sequence of Arp2 at the proposed Arp2-Arp3 interaction surface may be important for this (Beltzner and Pollard 2004). Actin-actin interaction surfaces are optimized to facilitate rapid polymerization; however, this surface on Arp2 is divergent from actin, and possibly repels Arp3, creating the requirement for an NPF to bridge and/or stabilize Arp2-Arp3 association. The two residues mutated in *arp2-7* are located in subdomain I (F127S) and subdomain II (F203Y) (Figure 2A). Phe127 is not predicted to make contacts with actin or other subunits of the Arp2/3 complex (Beltzner and Pollard 2004). However, Phe203, which corresponds to *Bos taurus* Phe205, is located at the pointed end of Arp2 and is predicted to be at the Arp3 interaction surface. Thus, substitution of Phe for Tyr (introducing a hydroxyl group) at this position in Arp2 may disrupt normal intermolecular repulsive forces between Arp2 and Arp3, thereby causing constitutive activation.

Arp2/3 complex activity must be strong and tightly regulated *in vivo*: Current models hold that the Arp2/3 complex must be tightly regulated *in vivo*, such that it remains inactive until the appropriate factors signal to

NPFs, which in turn stimulate Arp2/3 complex in the correct spatial and temporal manner. Direct comparisons in actin nucleation assays have shown that purified wild-type *S. cerevisiae* Arp2/3 complex is more constitutively active than bovine Arp2/3 complex (Rodal *et al.* 2005a). This could be interpreted to suggest that yeast can tolerate a slightly higher baseline of unregulated Arp2/3 nucleation activity than mammals. Alternatively, yeast may express cellular factors that actively dampen or suppress the baseline Arp2/3 complex nucleation activity. Here, we found that *arp2-7* increases the constitutive activity of yeast Arp2/3 complex, which causes defects in actin organization at low temperatures and arrest of cell growth at high temperatures. Recently, we described a mutant allele (*arc35-5*) of a different subunit p35/ARPC2 that is also partially constitutively active *in vitro* (Rodal *et al.* 2005a) and has defects in actin organization *in vivo*. Here we show that combining these two mutations in yeast is lethal, suggesting that there is a threshold of unregulated Arp2/3 complex activity above which cell viability is lost. Similarly, yeast can tolerate single mutations that each partially impair actin nucleation (*e.g.*, *arp2-1*, *arp2-2*, *arc35-6*, *las17*Δ, *myo3*Δ*myo5*Δ, and *pan1-101*), but most pairwise combinations of these alleles are lethal (Figure 1A and Table 2). Together, these observations demonstrate that the nucleation activity of Arp2/3 complex must be sufficiently potent *in vivo*, but also properly silenced in the absence of an activator.

We are extremely grateful to Avital Rodal for suggesting the use of *arp2* alleles to uncouple Arp2/3 regulation and for thoughtful advice throughout this work. We also thank Anya Goodman, Adam Martin, Omar Quintero-Monzon, Avital Rodal, David Shackelford, and Barbara Winsor for generously providing reagents and Heath Balcer, Fred Chang, Wei Guo, Avital Rodal, and Isabelle Sagot for helpful comments on the manuscript. This work was supported by a grant to B.G. from the National Institute of Health (GM63691).

LITERATURE CITED

Beltzner, C. C., and T. D. Pollard, 2004 Identification of functionally important residues of Arp2/3 complex by analysis of homology models from diverse species. J. Mol. Biol. **336:** 551–565.

Duncan, M. C., M. J. Cope, B. L. Goode, B. Wendland and D. G. Drubin, 2001 Yeast Eps15-like endocytic protein, Pan1p, activates the Arp2/3 complex. Nat. Cell Biol. **3:** 687–690.

Evangelista, M., B. M. Klebl, A. H. Tong, B. A. Webb, T. Leeuw *et al.*, 2000 A role for myosin-I in actin assembly through interactions with Vrp1p, Bee1p, and the Arp2/3 complex. J. Cell Biol. **148:** 353–362.

Goley, E. D., S. E. Rodenbusch, A. C. Martin and M. D. Welch, 2004 Critical conformational changes in the Arp2/3 complex are induced by nucleotide and nucleation promoting factor. Mol. Cell **16:** 269–279.

Goode, B. L., 2002 Purification of yeast actin and actin-associated proteins. Methods Enzymol. **351:** 433–441.

Goode, B. L., and A. A. Rodal, 2001 Modular complexes that regulate actin assembly in budding yeast. Curr. Opin. Microbiol **4:** 703–712.

Goode, B. L., A. A. Rodal, G. Barnes and D. G. Drubin, 2001 Activation of the Arp2/3 complex by the actin filament binding protein Abp1p. J. Cell Biol. **153:** 627–634.

Gourlay, C. W., H. Dewar, D. T. Warren, R. Costa, N. Satish *et al.*, 2003 An interaction between Sla1p and Sla2p plays a role in regulating actin dynamics and endocytosis in budding yeast. J. Cell Sci. **116:** 2551–2564.

Guthrie, C., and R. Fink, 1991 *Guide to Yeast Genetics and Molecular Biology* (Methods in Enzymology, Vol. 194). Academic Press, San Diego.

Higgs, H. N., L. Blanchoin and T. D. Pollard, 1999 Influence of the C terminus of Wiskott-Aldrich syndrome protein (WASp) and the Arp2/3 complex on actin polymerization. Biochemistry **38:** 15212–15222.

Huang, S., Y. Q. An, J. M. McDowell, E. C. McKinney and R. B. Meagher, 1996 The Arabidopsis thaliana ACT4/ACT12 actin gene subclass is strongly expressed throughout pollen development. Plant J. **10:** 189–202.

Huckaba, T. M., A. C. Gay, L. F. Pantalena, H. C. Yang and L. A. Pon, 2004 Live cell imaging of the assembly, disassembly, and actin cable-dependent movement of endosomes and actin patches in the budding yeast, Saccharomyces cerevisiae. J. Cell Biol. **167:** 519–530.

Jones, E. W., 2002 Vacuolar proteases and proteolytic artifacts in Saccharomyces cerevisiae. Methods Enzymol. **351:** 127–150.

Jonsdottir, G. A., and R. Li, 2004 Dynamics of yeast Myosin I: evidence for a possible role in scission of endocytic vesicles. Curr. Biol. **14:** 1604–1609.

Kaksonen, M., Y. Sun and D. G. Drubin, 2003 A pathway for association of receptors, adaptors, and actin during endocytic internalization. Cell **115:** 475–487.

Kelleher, J. F., S. J. Atkinson and T. D. Pollard, 1995 Sequences, structural models, and cellular localization of the actin-related proteins Arp2 and Arp3 from Acanthamoeba. J. Cell Biol. **131:** 385–397.

Kovar, D. R., J. R. Kuhn, A. L. Tichy and T. D. Pollard, 2003 The fission yeast cytokinesis formin Cdc12p is a barbed end actin filament capping protein gated by profilin. J. Cell Biol. **161:** 875–887.

Lechler, T., A. Shevchenko and R. Li, 2000 Direct involvement of yeast type I myosins in Cdc42-dependent actin polymerization. J. Cell Biol. **148:** 363–373.

Lees-Miller, J. P., G. Henry and D. M. Helfman, 1992 Identification of act2, an essential gene in the fission yeast Schizosaccharomyces pombe that encodes a protein related to actin. Proc. Natl. Acad. Sci. USA **89:** 80–83.

Li, R., 1997 Bee1, a yeast protein with homology to Wiscott-Aldrich syndrome protein, is critical for the assembly of cortical actin cytoskeleton. J .Cell Biol. **136:** 649–658.

Lila, T., and D. G. Drubin, 1997 Evidence for physical and functional interactions among two Saccharomyces cerevisiae SH3 domain proteins, an adenylyl cyclase-associated protein and the actin cytoskeleton. Mol. Biol. Cell **8:** 367–385.

Longtine, M. S., A. McKenzie, III, D. J. Demarini, N. G. Shah, A. Wach *et al.*, 1998 Additional modules for versatile and economical PCR-based gene deletion and modification in Saccharomyces cerevisiae. Yeast **14:** 953–961.

Machesky, L. M., S. J. Atkinson, C. Ampe, J. Vandekerckhove and T. D. Pollard, 1994 Purification of a cortical complex containing two unconventional actins from Acanthamoeba by affinity chromatography on profilin-agarose. J. Cell Biol. **127:** 107–115.

Madania, A., P. Dumoulin, S. Grava, H. Kitamoto, C. Scharer-Brodbeck *et al.*, 1999 The Saccharomyces cerevisiae homologue of human Wiskott-Aldrich syndrome protein Las17p interacts with the Arp2/3 complex. Mol. Biol. Cell **10:** 3521–3538.

Moreau, V., A. Madania, R. P. Martin and B. Winsor, 1996 The Saccharomyces cerevisiae actin-related protein Arp2 is involved in the actin cytoskeleton. J. Cell Biol. **134:** 117–132.

Pan, F., C. Egile, T. Lipkin and R. Li, 2004 ARPC1/Arc40 mediates the interaction of the actin-related protein 2 and 3 complex with Wiskott-Aldrich syndrome protein family activators. J. Biol. Chem. **279:** 54629–54636.

Pollard, T. D., 1984 Polymerization of ADP-actin. J. Cell Biol. **99:** 769–777.

Pollard, T. D., 1986 Rate constants for the reactions of ATP- and ADP-actin with the ends of actin filaments. J. Cell Biol. **103:** 2747–2754.

Quintero-Monzon, O., A. A. Rodal, B. Strokopytov, S. C. Almo and B. L. Goode, 2005 Structural and functional dissection of the Abp1 ADFH actin-binding domain reveals versatile in vivo adapter functions. Mol. Biol. Cell **16:** 3128–3139.

Robinson, R. C., K. Turbedsky, D. A. Kaiser, J. B. Marchand, H. N. Higgs *et al.*, 2001 Crystal structure of Arp2/3 complex. Science **294:** 1679–1684.

Rodal, A. A., M. Duncan and D. Drubin, 2002 Purification of glutathione S-transferase fusion proteins from yeast. Methods Enzymol. **351:** 168–172.

Rodal, A. A., A. L. Manning, B. L. Goode and D. G. Drubin, 2003 Negative regulation of yeast WASp by two SH3 domain-containing proteins. Curr. Biol. **13:** 1000–1008.

Rodal, A. A., O. Sokolova, D. B. Robins, K. M. Daugherty, S. Hippenmeyer *et al.*, 2005a Conformational changes in the Arp2/3 complex leading to actin nucleation. Nat. Struct. Mol. Biol. **12:** 26–31.

Rodal, A. A., L. Kozubowski, B. L. Goode, D. G. Drubin and J. H. Hartwig, 2005b Actin and septin ultrastructures at the budding yeast cell cortex. Mol. Biol. Cell **16:** 372–384.

Schwob, E., and R. P. Martin, 1992 New yeast actin-like gene required late in the cell cycle. Nature **355:** 179–182.

Tang, H. Y., J. Xu and M. Cai, 2000 Pan1p, End3p, and S1a1p, three yeast proteins required for normal cortical actin cytoskeleton organization, associate with each other and play essential roles in cell wall morphogenesis. Mol. Cell Biol. **20:** 12–25.

Toshima, J., J. Y. Toshima, A. C. Martin and D. G. Drubin, 2005 Phosphoregulation of Arp2/3 dependent actin assembly during receptor-mediated endocytosis. Nat. Cell Biol. **7:** 246–254.

Uruno, T., J. Liu, P. Zhang, Y. Fan, C. Egile *et al.*, 2001 Activation of Arp2/3 complex-mediated actin polymerization by cortactin. Nat. Cell Biol. **3:** 259–266.

Uruno, T., J. Liu, Y. Li, N. Smith and X. Zhan, 2003 Sequential interaction of actin-related proteins 2 and 3 (Arp2/3) complex with neural Wiscott-Aldrich syndrome protein (N-WASP) and cortactin during branched actin filament network formation. J. Biol. Chem. **278:** 26086–26093.

Wallar, B. J., and A. S. Alberts, 2003 The formins: active scaffolds that remodel the cytoskeleton. Trends Cell Biol. **13:** 435–446.

Weaver, A. M., A. V. Karginov, A. W. Kinley, S. A. Weed, Y. Li *et al.*, 2001 Cortactin promotes and stabilizes Arp2/3-induced actin filament network formation. Curr. Biol. **11:** 370–374.

Weaver, A. M., J. E. Heuser, A. V. Karginov, W. L. Lee, J. T. Parsons *et al.*, 2002 Interaction of cortactin and N-WASp with Arp2/3 complex. Curr. Biol. **12:** 1270–1278.

Welch, M. D., and R. D. Mullins, 2002 Cellular control of actin nucleation. Annu. Rev. Cell Dev. Biol. **18:** 247–288.

Wesp, A., L. Hicke, J. Palecek, R. Lombardi, T. Aust *et al.*, 1997 End4p/Sla2p interacts with actin-associated proteins for endocytosis in Saccharomyces cerevisiae. Mol. Biol. Cell **8:** 2291–2306.

Winter, D. C., E. Y. Choe and R. Li, 1999 Genetic dissection of the budding yeast Arp2/3 complex: a comparison of the in vivo and structural roles of individual subunits. Proc. Natl. Acad. Sci. USA **96:** 7288–7293.

Xu, Y., J. B. Moseley, I. Sagot, F. Poy, D. Pellman *et al.*, 2004 Crystal structures of a formin homology-2 domain reveal a tethered dimer architecture. Cell **116:** 711–723.

Communicating editor: M. Rose